RSC Advances

ROYAL SOCIETY OF CHEMISTRY

www.rsc.org/advances

RSC Advances

RSCPublishing

Communication

Nanoindentation Creep Behavior of Enamel Biological Nanocomposites

Cite this: DOI: 10.1039/x0xx00000x

Jing Zhang,[a,b] Chunbao Wang,[a,b] Fan Yang[a,b] and Chang Du[a,b*]

Received 00th January 2012,
Accepted 00th January 2012

DOI: 10.1039/x0xx00000x

www.rsc.org/

Abstract: Creep behaviour and mechanical properties of developing and mature porcine molar enamels in natural, lyophilized and burnt states were investigated by an AFM-attached nanoindentation system. The natural premature enamel has nearly 3 to 15 times more creep than mature enamel due to abundant organics and water contents. The natural mature enamel has the balanced mechanical properties, i.e., relatively high modulus and hardness with viscoelastic/viscoplastic deformation ability. After lyophilization, the mature enamel and those of late maturation stage had a significant increase in creep, while those of the transition stage with higher organics content showed slight but not statistically significant increase. The heat treatment to 600°C destroyed most organics and led to the crystal growth of HAp crystallites in enamel mineral. As a result, the modulus and hardness of the burnt samples were significantly increased while the ability of viscous deformation was compromised. The small amount of soft organic matrix between the nanoscale building units of hard mineral is thus one of important factors for the stress transfer as well as the viscous deformation. More significantly, water seems to play a vital role for the organics to fulfil its function and is essential in the design of the natural biological nanocomposite to resist external force. This study can provide a deeper understanding of relationship between enamel's composition, structure and mechanical performance.

1. Introduction

Biomineralized tissues (e.g., bone, tooth and shell) have long been the source of inspiration for advanced materials. They are both strong and tough due to unique nano-scale and micro-scale structures as well as inorganic and organic hybrid composition[1, 2, 3]. Unravelling the relationship between the composition, structure and mechanical property of these natural materials holds promise to develop biomimetic substitutes to repair ill or damaged hard tissues for human beings[4, 5].

Tooth enamel is a fascinating hard tissue with unique properties. Mature tooth enamel is generally considered as the hardest tissue in vertebrates and has long lifespan, though its primary composition is hydroxyapatite (HAp). Typical composition of mature tooth enamel is 96 wt% apatite mineral, 4 wt% water and organics[6]. It has a complex hierarchical structure from nano-scale to micro-scale[7]. In contrast, the immature developing enamel consists of substantial and variable content of water and proteinaceous matrix depending on the development stages[8, 9]. Enamel tissues of different developing stages thus provide unique platform to investigate the contribution of compositional and structural elements to the mechanical properties of the biocomposites, in particular their viscoelastic/viscoplastic behaviour.

Creep, described as a trend of permanent deforming due to stress in solid material, is of importance in demonstrating the viscous deformation property[10]. Recently, inelastic responses and creep behavior has been reported in mature enamel tissues using nanoindentation technique[11, 12]. As creep could be affected by chemical composition, structure and flaw of materials, it may help further investigate and explain enamel's excellent properties. Healthy human premolar tooth enamel displayed typical creep and backcreep behaviours, indicating both viscoelastic and viscoplastic properties similar to that of bone[12, 13, 14]. A double exponential function was described and the minor protein components together with the hierarchical structure were believed to play significant roles in determining the complex viscous deformation of enamel tissue[4, 12, 15]. Furthermore, G.A. Schneider *et al*[16] developed a viscous flow model of creep in enamel that considered the thin protein layer between the HAp crystallites as a viscous fluid. The model identified the main flow planes in the anisotropic enamel structure and explained the influence of the volume fraction of the apatite crystals.

In this study, premature enamels from porcine 2nd molar were investigated and compared with mature 1st molar enamel under nanoindentation system. The natural as well as the lyophilized and burnt samples were studied to illustrate the influence of water and organic matrix on the mechanical property of the various enamels. The results may give further understanding of formation mechanism of enamel's unique mechanical properties.

2. Experimental

2.1 Sample Preparation

Five premature porcine 2nd molars (labelled as S1 to S5) and a fully mature 1st molar (labelled as Control) were obtained from jaw bone of piglets in a local slaughterhouse. According to C. Robinson's classification[8, 17], S1 and S2 belong to the development stage 3 (the maturation stage) and S3 to S5 belong to an earlier stage 2 (the transition stage). The root of the samples was embedded with rosin and wax (1:1 w/w) in order to fix the samples on grind and polish machine (Phoenix Beta Grinder/Polisher, Buehler, USA) for polishing. The orientation was such that the cusp was almost vertical to the plate. Each sample was first grinded with 3000# silica abrasive paper until a small flat (about 1 mm^2) appeared, then polished with diamond polish paste for 5 minutes, following the order of 5μm, 2.5μm, 0.5μm and finally 0.05μm diamond suspension. Polished samples were treated with supersonic clean for about 5s with absolute ethyl alcohol[18]. Finally these samples were rinsed with water and briefly stored in 1X Hank's Balance Salt Solution (Invitrogen, USA) at the temperature of 4°C.

After the first round of nanoindentation test, the same samples were lyophilized (FD-5 series freeze dryer, Gold Sim, USA) for the second round of nanoindentation test. Afterwards, the samples were slowly heated to 600°C with a heating rate of 100°C per hour, kept for 2h and then slowly cooled down to room temperature. The third round of nanoindentation test was performed on the heat-treated samples.

2.2 Structural and compositional characterization

AFM (MFP-3D, Asylum Research, USA) was employed for the morphological characterization. The topographical observations were performed on the polished surface under either tapping mode with an Al-coated silicon probe (PPP-NCHR, NanoSensors, USA) or contact mode with an Au-coated silicon tip (ATEC-CONTAu, NanoSensors, USA).

Sufficient enamel tissue was scraped from premature sample and grounded into powders to extract mineral. Powders were then vibrated and ultrasonically dispersed in 0.1M phosphate buffers (pH=7.4) and 50mM Tris buffers (including 4M urea, pH=7.4, Double-helix, China), deionized water and 3% sodium hypochlorite, respectively. The dispersed enamel minerals were lyophilized thereafter for 48h and re-suspended in methanol for Transmission Electron Microscopy observation (JEM-2100HR, JEOL, Japan).

The enamel tissues near the flat area were scratched for the characterization with thermo-gravimetric analysis (TGA), Raman spectroscopy and X-ray diffraction (XRD). In order to characterize the content of organics and water of different enamel tissues, TGA (STA 499C, Netsch, Germany) was conducted on Control, S1, S3 and S4 samples from room temperature to 800°C in the N_2 atmosphere. The heating rate was 10°C/min. The Control and S1 sample was further characterized by Raman spectroscopy (LabRAM, HJY, France) at a wavelength of 532nm. The spectral region was 4000-50 cm^{-1}. The crystallographic change between natural and heated enamel of S1 was observed with XRD (X'Pert Pro, Panalytical, the Netherland). The test used Cu K_α radiation (λ=0.154nm) and a one-dimensional position-sensitive silicon strip detector. The data were collected with a step size of 0.033° and 2θ range from 10° to 90°.

2.3 Nanoindentation test

Nanoindentation was performed on the polished surfaces using AFM-attached nanoindentation system with a calibrated diamond Berkovich indenter. Before each indentation, an AFM image of interest area was obtained under contact mode. Then fast load-dwell-unload indentation was performed close to the central area of a prism. The applied force was 500μN and dwell time was 120s. The creep data were obtained from the force-indentation depth curves. For each sample, 10 indentations were performed with an interval of more than 5μm between each indentation area. An unpaired Student's *t*-test was applied to evaluate the significance of the differences between natural, lyophilized and heat-treated samples. A value of $p<0.05$ was considered as statistically significant.

Elastic modulus (E) and hardness (H) were obtained using Asylum Research MFP-3D software developed on the Igor Pro 6.21 platform. In this work, E and H were fitted with Oliver-Pharr model and calculated using following equations:

$$\frac{1}{E_c} = \frac{1-\nu^2}{E} + \frac{1-\nu_i^2}{E_i} \quad (1)$$

and

$$H = \frac{P_{\max}}{A_c} \quad (2)$$

where ν is the Poisson's ratio of sample, E_c is the reduced elastic modulus. For enamel, ν is typically 0.25. νi and Ei are Poisson's ratio and elastic modulus of the indenter tip. For Berkovich indenter used in this study, ν_i and E_i are 0.2 and 865GPa, respectively. P_{max} is the maximum load applied during nanoindentation test, and A_c is the projected contact area as a function of indentation depth hc:

$$A_c = 3\sqrt{3}h_c^2 \tan^2\theta \approx 24.5h_c^2 \quad (3)$$

All E and H data were presented as means ± standard deviation (SD).

3. Results and Discussion

3.1 Topographical observation

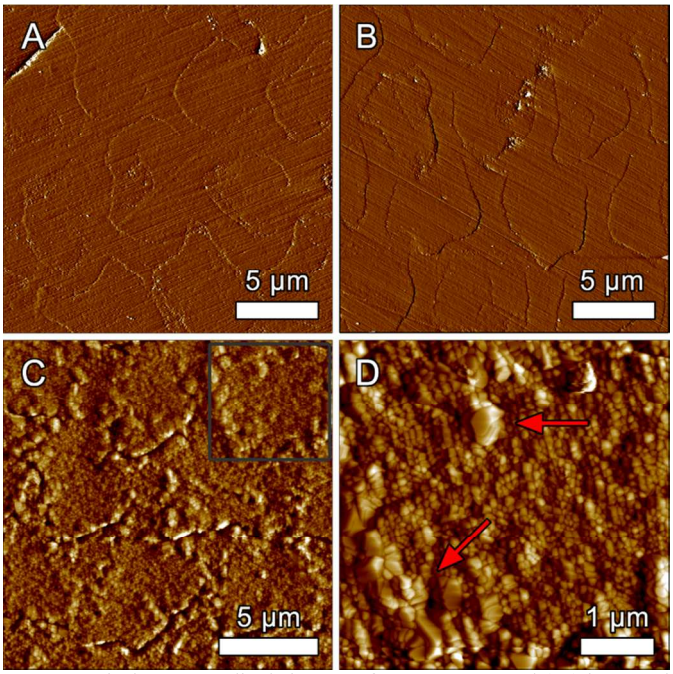

FIG.1: Typical AFM amplitude images of premature enamel (S1) in natural (A) and lyophilized (B) state under tapping mode, and deflection images after heat treatment (C, D) under contact mode. The test plane was perpendicular to cusp. (D) is the enlargement of the black box area in (C),

showing the cracks around the prism and obvious crystal growth (red arrows).

FIG.1 illustrates the surface morphology of the premature enamel (S1). Typical key-hole structure in the natural enamel can be clearly seen in FIG.1A. The surface roughness was about 3.1nm. A similar morphology was observed after lyophilization with a surface roughness of about 2.2nm as shown in FIG.1B. The periphery of the prism, or the "sheath" region, became slightly more obvious, which could be ascribed to the loss of water. In general, lyophilization seemed to introduce no significant change into surface topography.
After heat treatment at 600°C, premature enamel has significantly changed the morphology, as shown in FIG.1C and 1D. The surface roughness increased to about 21.8nm due to an obvious crystal growth, especially at the periphery of prisms. Cracks were noted mainly in the "sheath" region due to the loss of substantial amount of organics and water.

3.2 Compositional and structural characterization

TGA confirmed the decreasing contents of organics and water of the samples along with the development of enamel tissue, consistent with the classification of transition stage (S3 and S4), maturation stage (S1) and fully mature sample (Control), as shown in FIG. 2. The weight loss was observed in two temperature ranges. The removal of adsorbed water occurred up to about 200°C. A substantial decomposition of organic matrix and lattice water occurred from 200°C to 600°C. Typically the fully mature molar enamel had 5.8wt% of organic matrix and water. In contrast, the maturation stage and premature transition stage enamels had 6.5wt% (S1), 15.7wt% (S3) and 11.5 wt% (S4) organic matrix, respectively.

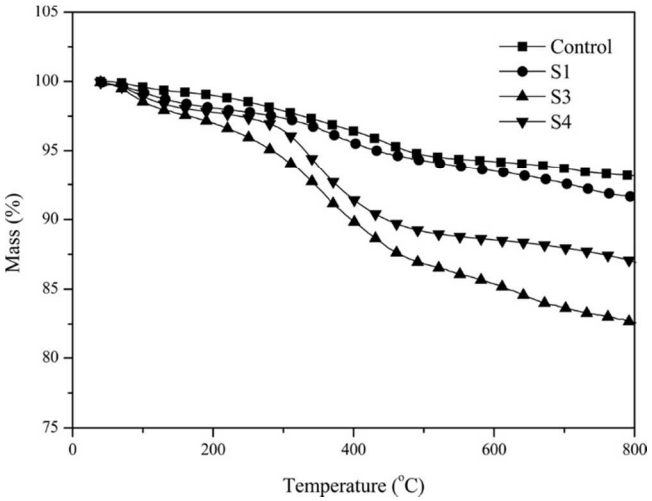

FIG. 2: TGA mass loss of Control, S1, S3 and S4 samples from room temperature to 800°C in nitrogen atmosphere.

Raman spectroscopy of fully mature enamel (Control sample) and premature S1 sample is shown in FIG. 3. The strongest band at 960cm^{-1} was attributed to ν1 stretching vibration mode of PO_4^{3-} in hydroxyapatite[19, 20]. Other bands assigning to ν2, ν3 and ν4 vibrating mode of phosphate are observed at 430cm^{-1}, 1045cm^{-1} and 590cm^{-1}, respectively[21, 22]. The relative intensity of 960cm^{-1} and 1045cm^{-1} bands of mature enamel is more intense than that of premature enamel. The organic matrix in S1 sample produced several significant bands at 1070cm^{-1}, 1450cm^{-1}, 1650cm^{-1} and 2935cm^{-1}, attributing to C-O stretching, C-H bending, Amide I stretching and C-H stretching vibration of CH_n groups, respectively[23]. The band at 3580cm^{-1} is attributable to OH ν1 stretching vibration or hydrogen bond, arising from water molecule within prism[24, 25]. Detailed observation from 1300cm^{-1} to 1800cm^{-1} is shown in inset of FIG. 3. It is clear that premature S1 enamel has more organic matrix than the mature enamel.

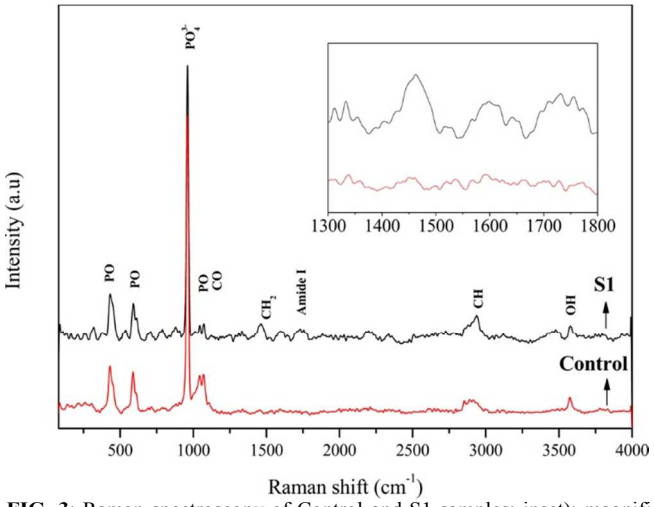

FIG. 3: Raman spectroscopy of Control and S1 samples; inset): magnified spectroscopy from 1300 to 1800cm^{-1}.

The XRD spectra of S1 sample in its natural state and after heat treatment are shown in FIG.4. Miler indices are assigned according to standard XRD PDF card No. 024-0033 for hydroxyapatite. The improved definition of (112) peak in the heat-treated sample is consistent to the morphological observation that heat treatment promoted crystal growth.

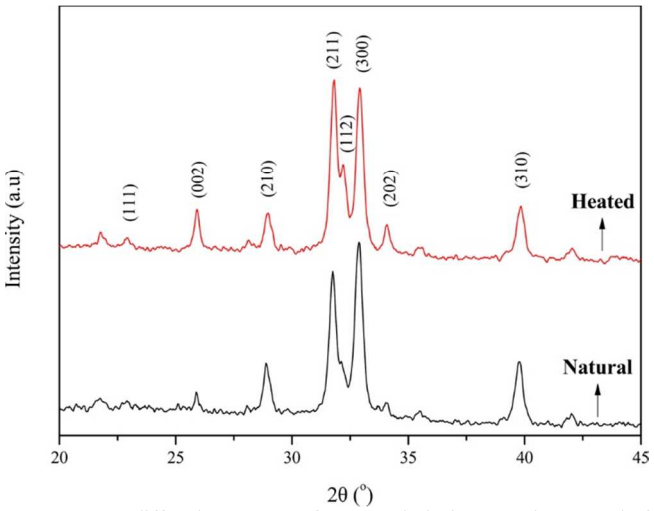

FIG.4: X-ray diffraction pattern of S1 sample in its natural state and after heat treatment.

3.3 Nanoindentation Creep

Indentation creep data are shown in FIG. 5A. Typical force-indentation curves of Control and S4 are shown in FIG. 5 (B) and (C). The natural premature enamels demonstrated 3 to 15 times more creep than mature enamel. In addition, the samples S3 to S5 have more creep than S1 and S2. The results are consistent with the maturation extent of these enamel tissues and their TGA study. It is evident that the mineral content is important for the tissue to resist to the external force.

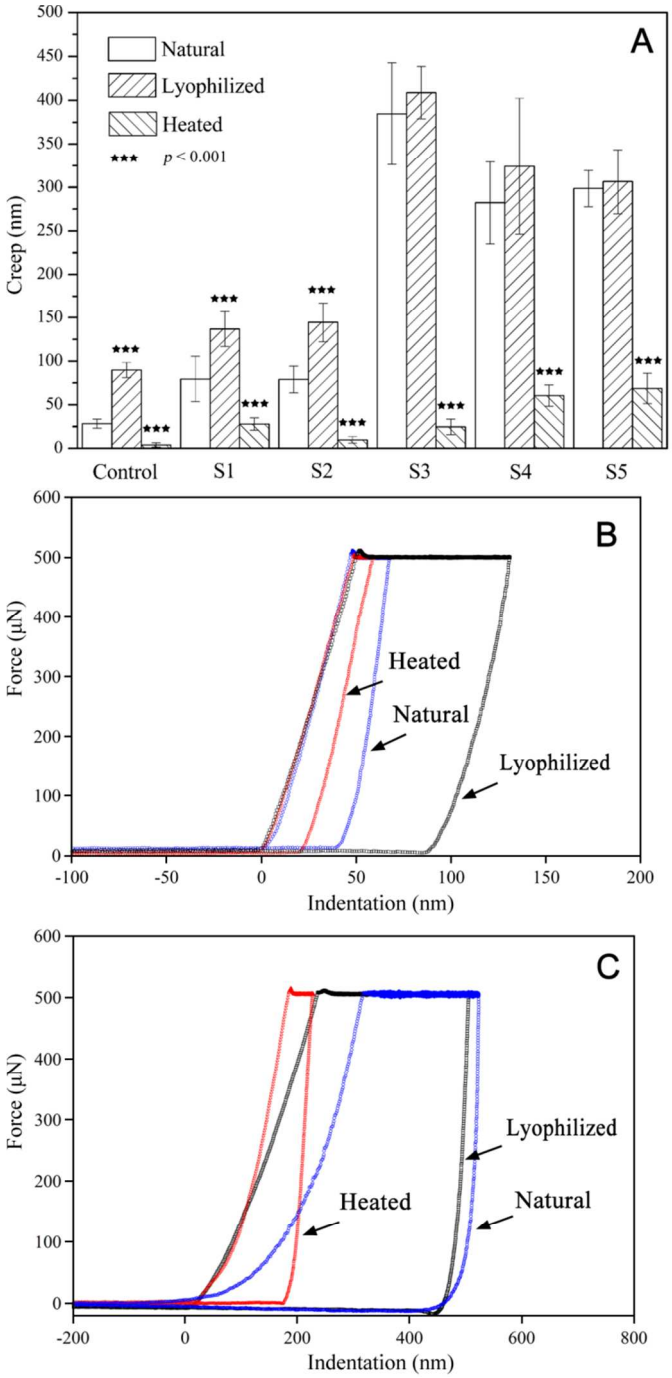

FIG. 5. (A) Nanoindentation creeps of all samples in different states at a load of 500μN and dwell time of 120s. The representative force-indentation depth curves of Control (B) and S4 (C) indicate that there are more creep and plastic deformation in premature enamel than fully mature enamel. (*** p<0.001 when the same sample was compared to its natural state)

It is interesting to note that water component played a vital role in the resistance of enamel tissue to external force, in particular in the fully mature sample (Control) and those of late maturation stage (S1, S2). After lyophilization, the Control and S1, S2 samples showed a significant increase in creep. Lyophilization led to the loss of water while the organic/inorganic components were reserved. The results suggested that water is crucial for the enamel tissue to distribute stress among the nanoscale crystallites. The loss of water hampered the stress transfer among the HAp crystallites as well as providing free space for HAp to deform or slide, thus promoting creep behaviour. The creep in S3 to S5 showed slight increase after lyophilization but not statistically significant, probably due to higher organics content in these samples.

After heat treatment, all of enamel samples exhibited significantly decreased creep (p<0.001). In mature enamel, creep reduced to 3.87±2.46nm which may be considered as thermal noise. The result manifested the pivotal role of small amount of organic component in the viscoelastic/viscoplastic property of mature enamel tissue. Heated premature enamels also showed much less creep comparing with results before any treatment. AFM observation as shown in FIG. 1 (C) and (D) has suggested that heat treatment promoted crystal growth within and around prism. As a result, the free spaces between the crystallites may have been enclosed or entirely disappeared. Direct stress transfer across the interface of neighbouring HAp crystallites enhanced the resistance of the entire structure to the external force, while significantly reducing the ability to the plastic deformation. From force-indentation curves, the area enclosed by loading, dwelling and unloading segments is defined as plastic work (W_P)[26]. It's evident that the natural premature enamel possesses more W_P than mature enamel. After unloading, there was more plastic deformation in premature enamels. Furthermore, the heat treatment significantly reduced the W_P of the same sample.

3.4 Elastic modulus and Hardness

TABLE I and II show the modulus (E) and hardness (H) of all samples in different conditions.

TABLE I. Elastic modulus of each sample (GPa)

	Natural	Lyophilized	Heated
Control	83.91 ± 9.90	24.84 ± 2.60	124.41 ± 16.18
S1	25.25 ± 9.35	19.27 ± 5.14	81.51 ± 12.31
S2	20.28 ± 8.27	23.29 ± 3.63	153.02 ± 21.38
S3	8.90 ± 1.20	8.84 ± 1.80	72.39 ± 16.18
S4	18.25 ± 3.87	10.54 ± 1.77	28.38 ± 3.68
S5	16.74 ± 1.76	14.87 ± 3.17	16.46 ± 4.19

TABLE II. Hardness of each sample (GPa)

	Natural	Lyophilized	Heated
Control	5.63 ± 1.52	1.2 ± 0.26	-
S1	1.06 ± 0.67	0.59 ± 0.28	-
S2	0.75 ± 0.53	0.69 ± 0.20	-
S3	0.11 ± 0.04	0.10 ± 0.02	-
S4	0.13 ± 0.04	0.12 ± 0.04	1.39 ± 0.46
S5	0.11 ± 0.02	0.15 ± 0.04	1.42 ± 0.60

E and H of mature enamel were close to the reported data for human mature molar enamel[27, 28, 29]. In contrast, premature enamel showed significantly lower modulus and hardness. After lyophilization, E and H of mature enamel decreased significantly by about 68% and 78%, respectively. This further

confirmed the pivotal role of water in the mechanical properties of mature enamel. For premature samples, a slight but statistically insignificant reduction in E and H can be noted due to the loss of water. The heat treatment led to a drastic increase in elastic modulus and hardness of all samples. Elastic modulus of the burnt mature sample and S2 reached to that of HAp single crystal[30]. The hardness data for the burnt mature to S3 enamels exceeded that of pure HAp and were not reliable, partly because the heat treatment increased the surface roughness, leading to a relatively large error in calculating the contact area. Nevertheless, the elastic modulus and hardness for burnt S4 and S5 samples present an obvious increase.

3.5 Viscosity of Organics

The effective viscosity of the organics η_{eff} under constant load P in enamel tissue was calculated from the equation below[16]:

$$\eta_{eff} = \frac{\gamma_c (1-\upsilon) Pt}{g k_c \delta_{creep}^2} \quad (4)$$

where γ_c and g are geometrical parameters of indenter. For a standard Berkovich indenter, γ_c is 1.2 and g is 24.5. k_c is taken as 0.46 according to Sakai and Shimizu[31]. Based on the creep data (δcreep) from force-indentation plot, the calculation results for P=500μN and t=120s are summarized in TABLE III.

TABLE III. The effective viscosity of the organics in enamels ($\times 10^{10}$Pa·s)

	Natural	Lyophilized
Control	712	71.6
S1	90.9	30.8
S2	92.4	27.5
S3	3.89	3.44
S4	7.22	5.47
S5	6.45	6.12

The calculated η_{eff} in fully mature enamel (Control) and late maturation stage enamels (S1 and S2) was higher than the premature transition stage samples (S3 to S5). The value for the premature enamel was two orders of magnitude lower than that for the mature enamel. However, the η_{eff} of Control, S1 and S2 enamels significantly decreased after lyophilization. Particularly, there was one order of magnitude decrease for the mature enamel. In contrast, the η_{eff} of the premature S3 to S5 enamels remained nearly unchanged before and after lyophilization.

It is known that massive degradation of the enamel organic matrix components is concomitant with the growth of crystals during the development of enamel tissue. FIG.6 (A) showed the TEM image of enamel crystallites extracted from the premature tissue. A typical plate-like morphology was noted. FIG.6 (B) shows a schematic of single HAp crystallite with the surrounding space for organics and water. The volume fraction of organics and water in enamel can thus be estimated using equation:

$$V_f = \frac{(x+h_1)(y+h_2)(z+h_3) - xyz}{(x+h_1)(y+h_2)(z+h_3)} \quad (5)$$

For the mature enamel, the HAp crystallites are simplified as rod-like according to Schneider et al[16] with the dimension x=y=50nm, z=500nm, and h_1=h_2=h_3=2nm. It gives a V_f of 8 vol% for mature enamel. Assuming the total volume doesn't change with crystal growth, dimension x and z in the premature enamel were taken as the same as in mature enamel. The aspect ratio of width to thickness is taken as 2:1 to reflect the plate-like morphology of HAp in premature enamel. The dimensions for the premature HAp subunit were thus approximated as 50nm, 25nm, 500nm, 2nm, 27nm and 2nm for x, y, z, h_1, h_2 and h_3. Calculation showed that the V_f of premature enamel under this model is 53.96 vol%.

The viscosity data for the premature samples were similar to the calculation on amelogenesis imperfecta infected hypomineralized teeth that higher volume contents of liquid phase (organics and water) significantly decreased the effective viscosity[16, 32]. Furthermore, our data suggested that the organic phase can effectively provide the viscosity even without the presence of water. This observation is consistent with the fact that the majority of proteinous organics in the developing enamel are amelogenins with hydrophobic nature[9]. For the mature enamel, however, water appeared to play significant role in ensuring a high viscosity of the organic phase. Schneider *et al*[16] concluded that the creep deformation of the mature enamel is mainly attributed to the viscous flow of the protein layer in the plane perpendicular to the long axes of HAp crystallites. Our data further suggested that water is essential for the flow of this thin protein layer.

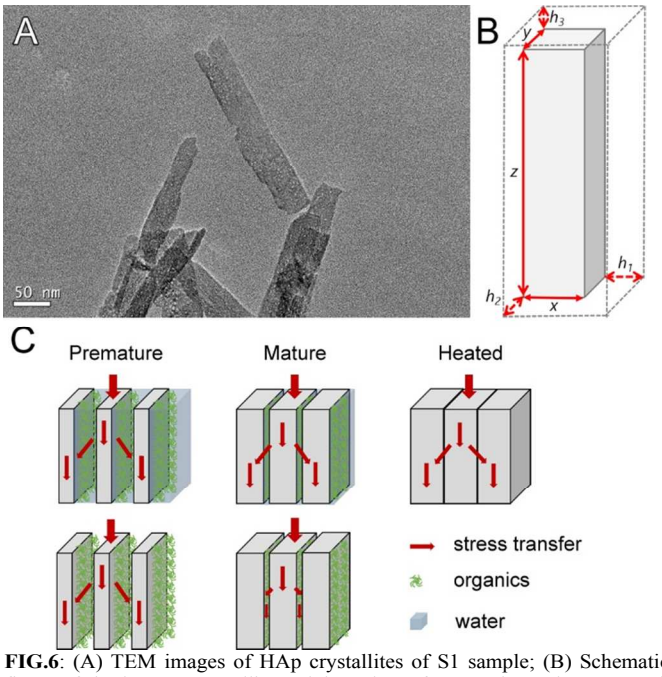

FIG.6: (A) TEM images of HAp crystallites of S1 sample; (B) Schematic figure of single HAp crystallite and the volume for organics and water. Dash line indicates the entire unit while solid line indicates HAp part. (C) Stress transfer model in premature, mature and heated enamels under nanoindentation.

Ji and Gao have established a tension–shear chain model to analyze the tensile strength and the viscoelastic properties of the protein-mineral nanostructure of biological materials[4]. They suggested that load transfer is largely accomplished by the high shear zones of protein between the long sides of mineral platelets. Adapted from this model, the stress transfer in different enamel samples under the current nanoindentation conditions was proposed as shown in FIG.6 (C). Both of the mineral platelets, organics content and water are important for the mechanical property of this biological nanocomposite. The

mineral platelets undertake the most compressive stress and the organic matrix is important for the stress transfer and re-distribution between adjacent minerals. Significantly, water is essential for the small amount of organics to fulfill its function. When the mature enamel is burnt (600^{o}C) to eliminate all the organics, the crystal growth leads to the direct contact of the hard mineral platelets. The modulus and hardness are significantly increased while the ability of viscoelastic/viscoplastic deformation is compromised.

4. Conclusions

In summary, we demonstrate that premature enamel has significant creep behavior than mature enamel due to abundant organics and water between HAp crystals. The mature enamel has the balanced mechanical properties, i.e., relatively high modulus and hardness with viscoelastic/viscoplastic deformation behavior. The small amount of soft organic matrix between the nanoscale building units of hard mineral is one of important factors for the stress transfer as well as the viscous deformation. Significantly, water plays a vital role for the organics to fulfill its function and is essential in the design of the natural biological nanocomposite to resist external force. This study may provide a deeper understanding of relationship between enamel's composition, structure and mechanical performance.

Acknowledgements

This work was financially supported by National Basic Research Program of China (2012CB619100), the National Natural Science Foundation of China (51072056), the Program for Changjiang Scholars and Innovative Research Team in University (IRT 0919), the 111 Project (B13039) and Key Grant of Chinese Ministry of Education (313022).

Notes and references

[a]School of Materials Science and Engineering, South China University of Technology, Guangzhou, Guangdong, China PR.
[b]National Engineering Research Center for Tissue Restoration & Reconstruction, South China University of Technology, Guangzhou, Guangdong, China PR.
*Email：duchang@scut.edu.cn

1 I. Jäger and P. Fratzl, *Biophys. J.*, 2000, **79**, 1737-1749.
2 S. Habelitz, S. J. Marshall, G. W. Marshall and M. Balooch, *Arch. Oral Biol.*, 2001, **46**, 173-183.
3 S. Younis, Y. Kauffmann, L. Bloch and E. Zolotoyabko, *Cryst. Growth Des.*, 2012, **12**, 4574-4579.
4 B. Ji and H. Gao, *J. Mech. Phys. Solids*, 2004, **52**, 1963-1990.
5 B. Bar-on and D. H. Wagner, *J. Biomech.*, 2012, **45**, 672-678.
6 K. E. Healy, in *Handbook of Biomaterial Properties*, ed. J. Black and G. Hastings, Springer, USA, 1st edn., 1998, ch. 3, pp. 24-39.
7 F. Z. Cui and J. Ge, *J. Tissue Eng Regen Med*., 2007, **1**, 185-191.
8 J. Kirkham, C. Robinson, J. A. Weatherell, A. Richards, O. Fejerskov and K. Josephsen, *J. Dent. Res.*, 1988, **67**, 1156-1160.
9 A. G. Fincham, J. Moradian-Oldak and J. P. Simmer, *J. Struct. Biol.*, 1999, **126**, 270-299.
10 S. Murakami and N. Ohno, in *Creep in Structures*, ed. ARS Ponter and DR Hayhurst, 3rd edn., International Union of Theoretical and Applied Mechanics, Leicester, 1980, pp. 422-444
11 L. H. He and M. V. Swain, *J. Dent.*, 2007, **35**, 431-437.
12 L. H. He and M. V. Swain, *J. Biomed. Mater. Res. A*, 2009, **91A**, 352-359.
13 T. Goto, N. Sasaki, K. Hikichi, *J. Biomech.,* 1999, , 93-97.
14 N. Sasaki, M. Yoshikawa, A. Enyo, *J. Biomech*., 1993, **26**, 1369-1376.
15 I. R. Spears, *J. Dent. Res.*, 1997, **76**, 1690-1697.
16 G. A. Schneider, L. H. He, M. V. Swain, *J. Appl. Phys.*, 2009, **103**, DOI: 10.1063/1.2827987.
17 C. Robinson, J. Kirkham, J. A. Weatherell, A. Richards, K. Josephsen and O. Fejerskov, *Caries Res.*, 1988, **22**, 321-326.
18 J. Ge, F. Z. Cui, X. M. Wang, H. L. Feng, *Biomaterials*, 2005, **26**, 3333-3339.
19 L. H. He and M. V. Swain, *J. Dent.*, 2009, **37,** 596-603.
20 Y. Liu and C. Y. S. Hsu, *J. Dent.*, 2007, **35**, 226-230.
21 G. Penel, G. Leroy, C. Rey and E. Bres, *Calcified Tissue Int.*, 1998, **63**, 475-481.
22 K. A. Schulze, M. Balooch, G. Balooch, G. W. Marshall and S. J. Marshall, *J. Biomed. Mater. Res. A*, 2004, **69A**, 286-293.
23 A. Carden and M. D. Morris, *J. Biomed. Opt.*, 2000, **5**, 259-268.
24 J. Gómez-Morales, M. Iafisco, J. M. Delgado-López, S. Sarda, C. Drouet, *Prog. Cryst. Growth Ch.*, 2013, **59**, 1-46.
25 V. Uskoković and D. P. Uskoković, *J. Biomed. Mater. Res. B*, 2011, **96B**: 152-191.
26 K. K. Jha and N. Suksawang, *J. Mater. Res.*, 2013, **28**, 789-797.
27 J. Zhou and L. L. Hsiung, *J. Biomed. Mater. Res. A*, 2007, **81A**, 66-74.
28 L. H. He, N. Fujisawa and M. V. Swain, *Biomaterials*, 2006, **27**, 4388-4398.
29 S. Park, D. H. Wang, D. Zhang, E. Romberg and D. Arola, *J. Mater. Sci. Mater. Med.,* 2008, **19**, 2317-2324.
30 S. Saber-Samandari and K. A. Gross, *Acta Biomater.*, 2009, **5**, 2206-2212.
31 M. Sakai and S. Shimizu, *J. Non-Cryst. Solids,* 2001, **282**, 236-247.
32 J. T. Wright, S. C. Chen, K. I. Hall, M. Y. Yamaguchi and J. W. Bawden, *J. Dent. Res.*, 1996, **75**, 1936-1941.

Organic matrix and water are essential factors for enamel biological nanocomposite to resist external force as revealed by nanoindentation creep test.